GRANT
NT-74-CR
171490
P.36

FINAL REPORT

TITLE: **Ultra-High Resolution Water Window X-Ray Microscope Optics Design and Analysis**

P.I.: David L. Shealy, Ph.D.
Department of Physics
1300 University Blvd., Rm. 310
Univ of Alabama at Birmingham
Birmingham, AL 35294-1170
205-934-8068
FAX: 205-934-8042
INTERNET: shealy@uabphy.phy.uab.edu

CONTRACT NO.: NASA-PO-H13006D

PERIOD OF CONTRACT: March 18, 1992 - June 17, 1993

DATE: June 25, 1993

Distribution:

AP29-Q-Amy Williams	(1*)
CN22D	(5)
AT01	(1)
CC01/Intellectual Prop. Counsel	(1)
EM14-46/McCranie	(1)
COTR (ES52-R.B. Hoover) Marshall Space Flight Center, AL 35812	(5*)
NASA Center for AeroSpace Information Attn: Accessioning Department 800 Elkridge Landing Road Linthicum Heights, MD 21090	(1 + repro.)

* Copy of letter of transmittal plus copy of Technical Report

Final Report 1993: Ultra-High Resolution Water Window X-Ray Microscope Optical Design and Analysis Purchase Order No. H-13006D

D. L. Shealy and C. Wang
Department of Physics
310 Campbell Hall
University of Alabama at Birmingham
Birmingham, AL 35294-1170
Internet: shealy@uabphy.phy.uab.edu

June 25, 1993

Abstract

This project has been focused on the design and analysis of an ultra-high resolution water window soft-x-ray microscope. These activities have been accomplished by completing two task contained in the Statement of Work of this contract. The new results from this work confirm (1) that in order to achieve resolutions greater than three times the wavelength of the incident radiation, it will be necessary to use aspherical mirror surfaces and to use graded multilayer coatings on the secondary in order to accommodate the large variations of the angle of incidence over the secondary when operating the microscope at numerical apertures of 0.35 or greater; (2) that surface contour errors will have a significant effect on the optical performance of the microscope and must be contolled to a peak-to-valley variation

of 50 – 100 Å and a frequency of 8 periods over the surface of a mirror; and (3) that tolerance analysis of the spherical Schwarzschild microscope has been shown that the water window operations will require 2 – 3 times tighter tolerances to achieve a similar performance for operations with 130 Å radiation. These results have been included in a manuscript entitled "Prospects for Achieving Ultra-High Resolution with a Multilayer, Two-Mirror Microscope," which is enclosed in the Appendix of this report.

1 Introduction:

In support of the NASA/MSFC Advanced Water Window X-ray Microscope effort, this work addressed two task. Task 1 (Advanced Water Window Imaging X-Ray Design) focused on determination of analytical and numerical equations for the Head microscope mirror surfaces in a form which can be used by conventional optical design codes, manufacturing, and testing. Task 2 (Tolerance Analysis of Soft-X-Ray Microscope) proposed to analyze mirror surface figure errors to determine whether the state-of-the-art mirror fabrication and testing will be adequate to enable the Head configuration of the Water Window Microscope to achieve resolution less than 100 Å. The manpower funded by this contract was allocated equally between these two Task, which were completed and have been presented to the NASA/MSFC Technical Coordinator of this project (R. B. Hoover) and were part of an invited presentation given by the PI to *Soft X-Rays in the 21st Century Conference*, February 10-13, 1993, Provo, Utah. Further, the Editor of the Journal of Soft X-Ray Science and Technology has invited the PI to submit a manuscript based on this work for publication. A draft of this manuscript is included in the Appendix of this report. The reader of this report is encouraged to read the manuscript contained in the Appendix first. Then, results, recommendations and conclusions of this project are presented in the next two sections of this report.

2 Results

Figure 1 presents a geometrical configuration of the Head-Schwarzschild microscope. When configuring a reflecting microscope system, the magnifica-

tion is normally determined by the object and detector resolutions. Equations 1 - 3 from the Appendix enable one to evaluate the Schwarzschild microscope parameters when the magnification, m, and radius of curvature of the secondary, R_2, are given. Table 1 from Appendix presents a tabulation of Schwarzschild microscope parameters when $R_2 = 10cm$ and m ranges from 2 to $100x$. When alternate values of R_2 are used, all spatial dimensions scale linearly with R_2. Section 2 of the Appendix presents a complete discussion of the performance and system parameters of a spherical Schwarzschild microscope including some relationships between NA, magnification, diameter of the primary mirror, radius of curvature of the secondary mirror, and the total length of the microscope. To achieve resolutions better than a spherical Schwarzschild microscope of 3.3λ for a perfectly aligned and fabricated system, it is necessary to use aspherical surfaces to control higher-order aberrations.

Using the equations presented in section 3 of the Appendix, data for the aspherical mirror surfaces of a Head microscope can be evaluated when the magnification and the spacings between the object and primary, image and secondary, and the two mirror surfaces are given. Using a linear least squares fitting technique, the mirror surface data can be fitted by surface equations of the form

$$z(h) = \frac{ch^2}{1 + \sqrt{(1 - c^2h^2)}} + \sum_{i=4,6}^{i\,\max} A_i h^i \qquad (1)$$

where c is the vertex curvature, h is the height of a ray from the optical axis, A_i are the aspherical deformation coefficients, which range in number depending of the fitting approach. For the aspherical coefficients presented in Table 2 of the Appendix, $i\,\max = 6$, and two aspherical deformation terms were considered in this fit. This system represents perhaps the simplest description of a Head microscope with $NA = 0.35$ that provides diffraction limited performance, and thus, should be a primary system to fabricate and test.

Although it has been demonstrated that the Head microscope can be designed to achieve diffraction limited performance over a large numerical aperture and the Head surfaces can be fitted very accurately, it can not be assumed that a Head microscope can actually be built to operate at these high numerical apertures, since the aspherical surfaces will require very accurate manufacturing of the surface contour. In addition to the system toler-

ances for alignment, analysis of the surface manufacturing tolerance become very important for soft-x-ray systems. In order to investigate the effects of the manufacturing process of optical surfaces on the performance of the designed system, some numerical simulations have been done. Based on an understanding of the manufacturing process, assume that the manufacturing process introduces some errors into the mathematically well fitted surfaces. Then, one can assume that a real surface can be described by the following formula:

$$z = f(x,y) + \delta(x,y) \tag{2}$$

where $f(x,y)$ represents the ideally fitted surface and $\delta(x,y)$ describes the manufacturing errors introduced into the surface contour.

For manufacturing a sysmmetric surface, the surface substrate usually is rotated about the symmetry axis while the cutting tool is milling on the surface, and the cutting tool should also be moved back and forth along the radial direction to cover the entire surface. Thus, it is reasonable to assume that the manufacturing surface errors are rotationally symmetric around the surface. In this simulation work, an approximately linear model for the manufacturing surface errors has been used and can be written as follows:

$$\delta(r) = kr[1 + c\sin(2\pi f_0 r)] \tag{3}$$

where $k = (Error_{\max})/r_{\max}$ is a constant that gives the maximum contour error on the surface, the constant c measures the contribution of rotational error effects, and f_0 gives the frequency of these rotational error effects. Figures 11-12 from the Appendix show the surface error functions with different values of parameters and the appropriate sine wave MTF for each case. It can be seen from Figs. 11-12 that the simulated surface errors contribute significantly to the system performance even though the maximum error value is only a quarter of wavelength.

3 Recommendations and Conclusions:

This investigator recommends that NASA fabricate a $30x$ Head-Schwarzschild microscope configured as listed in Table 2 of Appendix. The substrate fabrication and test of this system appear to be more promising than the other

systems considered. In order to realize the resolution enhancement potential of these fast Head microscope, it will be necessary to use a divergent x-ray source with cone half-angle of at least 20°, which suggest that a laser plasma system would be a good source configuration to enable the fast microscope to achieve the ultra high resolution of the diffraction limited performance of 1.4λ. Tolerance analysis of the spherical Schwarzschild microscope has shown that the water window operations will require $2-3$ times tigher tolerances to achieve a similar performance for operations with 130 Å radiation. Surface contour errors have been shown to have a significant impact on the optical performance and must be controlled to a peak-to-valley variation of $50-100$ Å and frequency of 8 periods over the surface of a mirror.

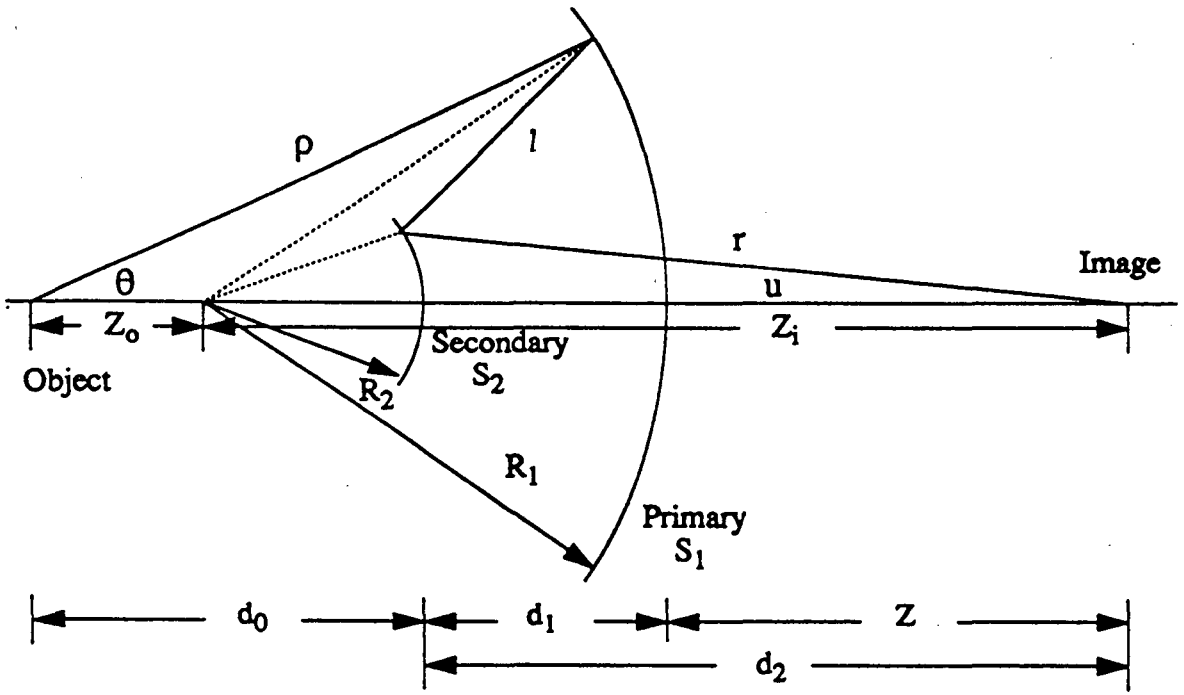

Figure 1: Geometrical configuration of a Head-Schwarzschild microscope.

APPENDIX

Prospects for Achieving Ultra-High Resolution with a Multilayer, Two-Mirror Microscope

David L. Shealy, Cheng Wang
Department of Physics
University of Alabama at Birmingham
Birmingham, AL 35294-1170

Richard B. Hoover
Space Science Laboratory
NASA/Marshall Space Flight Center
Huntsville, AL 35812

ABSTRACT

Promoted by the successful application of multilayer coated optics in soft x-ray imaging experiments in solar physics and projection lithography, several groups have designed, analyzed, fabricated, and are testing Schwarzschild multilayer, soft x-ray microscopes. Simulations have indicated that diffraction limited performance of a spherical Schwarzschild microscope operating near 100 Å will be limited to systems with a small numerical aperture of approximately 0.15 and a corresponding resolution, based of the Rayleigh criterion, of 3.3 times the wavelength of the incident radiation. In principle, a two aspherical mirror Head microscope, which satisfies the constant optical path length condition and the Abbé Sine Condition, should achieve diffraction limited performance for very large numerical apertures. However, surface contour errors and variation of the angle of incidence over the multilayer substrates become significant factors in degrading system resolution and must be controlled. For a $30x$ reflecting microscope with a numerical aperture ranging from 0.15 to 0.35, the effects on resolution of surface contour errors, tilts and misalignments of the optics have been studied. Graded spacing of the multilayer coatings on the mirror substrates are required to enable operation of a fast, two-mirror microscope. These studies coupled with an assessment of substrate and multilayer coating technologies form the basis for projecting the prospects of achieving ultra-high resolution with a multilayer, two-mirror microscope operating with soft x-rays.

1 Introduction

Due to the vacuum environment of a sample, conventional electron microscopes can not be used to investigate biological samples under natural conditions. X-ray microscopes provide a different way of studying samples with a resolution of several hundred angstroms.[1, 2, 3] Although diffractive zone plates[4] can be used to focus x-rays in a microscope with a resolution of about 300 Å, there are some problems, such as, low diffraction efficiency and the high cost of making the zone plates, which seem to constrain zone plate x-ray microscopes from achieving resolutions of less than 200 Å. The development of multilayer coatings[5, 6] provides the possibility of using multilayer coated mirrors for soft-x-ray microscopy studies with very high resolutions.

An important field for using high resolution soft-x-ray microscopy is cell biology. Many biological samples contain carbon based molecules in an aqueous environment. The water window[7] refers to the soft-x-ray wavelength region of 23.6 – 43.6 Å in which water is relatively transparent and carbon is highly absorptive. This provides the possibility of studying the structure of DNA and macromolecules within living cells. In order to study microscopic features of biological objects, a multilayer coated, reflecting microscope has been proposed for use within the water window,[8, 9] where one would like to resolve features smaller than 100 Å.[10] For a reflecting microscope, this means that a numerical aperture of about 0.4 or greater is required to enable the system to achieve resolutions less than 100 Å.

The Schwarzschild two-mirror system[11, 12] has been used for many microscopy and projection lithography applications over a wide range of the electromagnetic spectrum. Recently, the spherical Schwarzschild optics coated with multilayers have been used in soft-x-ray microscopy applications[8, 13, 14, 15, 16] and for projection lithography[17, 18] where linewidths of 500 Å have been written on photoresist by AT&T Bell Labs. While operating within the 100 – 200 Å region, diffraction limited performance has been obtained for a small numerical aperture ($NA \leq 0.16$) and over a small field of view.

In an effort to provide capabilities for using alternate configurations of two-mirror microscopes while only using third-order designs, Hannan[19] has presented a general analysis of a two conical mirror relay system which corrects third-order spherical aberration, coma, and astigmatism. The concentric, spherical Schwarzschild system is a special case of Hannan's formulation. Hannan's approach enables one to construct a two-mirror microscope where the two conical mirrors are used to overcome the constraint of concentric, spherical mirrors required in the conventional Schwarzschild system. However, the Hannan system does not provide for any higher order correction of aberrations and would likely not function well with a large NA. In order to increase the resolution, one can decrease the operating wavelength and/or increase the NA. To increase the NA and to control aberrations such that diffraction limited performance can be achieved, the authors have proposed using the aspherical Head microscope design.[20, 21]

A. K. Head[22] has used the aplanatism conditions of constant optical path length and the Abbé Sine condition rays to set up differential equations for determining the surface shapes of a two-mirror imaging system such that all orders of spherical aberration and coma are zero. This

means that the Head microscope should provide near diffraction limited performance for very large numerical apertures over a small field of view. Analytical solutions of these two differential equations have been obtained but can not readily be used by conventional optical design codes to determine the performance of a Head microscope.

In this paper, the design and analysis of the performance of a Schwarzschild microscope is reviewed. Then, a parametric study for a spherical Schwarzschild microscope has evaluated the relationships between NA, magnifications, total system length, mirror radii and diameters. In section 3, an analysis of the characteristics of the aspherical surfaces of a Head-Schwarzschild microscope are presented, including a discussion of fitting a conic function plus aspherical deformation terms to the mirror surface data. The optical performance of a fast Head microscope has been analyzed by conventional optical design codes. Analyses of the Head surface shapes and of the variation of the angles of incidence over the mirror surfaces have been performed to determine whether current optical substrate and multilayer coating technologies will permit construction of a very fast Head microscope which may provide resolution approaching that of the wavelength of the incident radiation. This paper concludes with a discussion of the tolerance analysis of a Schwarzschild microscope operating at 40 Å and 130 Åand of the surface figure errors of the aspherical Head mirrors.

2 Schwarzschild Configuration

A third-order aplanatic design of a reflecting microscope can be made from two concentric spherical mirrors as shown in Fig. 1, if the mirror radii satisfy the Schwarzschild condition:

$$\frac{R_2}{R_1} = \frac{3}{2} - \frac{R_2}{Z_0} \pm \sqrt{\frac{5}{4} - \frac{R_2}{Z_0}} \tag{1}$$

where R_1 and R_2 are the radii of curvature of the primary and secondary mirrors, Z_0 is the distance from the object point to the center of curvature of the two mirrors, and the + sign in Eq. 1 is used when the magnification is greater than 5. Using paraxial optics relationships, the magnification of a spherical Schwarzschild microscope can be written as

$$m = \frac{-R_1 R_2}{(2R_1 Z_0 - R_1 R_2 - 2R_2 Z_0)}. \tag{2}$$

For a derivation and more discussion of the Schwarzschild condition, Eq. 2 and some ray tracing analyses, see Ref. [12]. It has also been shown[23] that a spherical Schwarzschild microscope does not have any third-order astigmatism while also satisfying the third-order aplanatism conditions. A more convenient relationship for computing microscope system parameters in terms of the system magnification (m) is obtained by elimenating R_1 in Eqs. 1 and 2 to obtain

$$\frac{R_2}{Z_0} = \frac{-m(m-1) + m\sqrt{(m-1)^2 + 4(m+1)^2}}{(m+1)^2} \tag{3}$$

where R_1 can now be evaluated as a function of m from Eqs. 1 and 3. Using the mirror equation and Eqs. 1 - 3, one can evaluate the data in Table 1, which gives the Schwarzschild system parameters for a range of magnifications where $L(= Z_0 + Z_i)$ is the total length of a microscope and $Z(= Z_i - R_1)$ is the distance from the vertex of the primary mirror to the image plane. The data in Table 1 can be scaled linearly. For example, to obtain the system parameters of a microscope with a secondary radius of curvature of 5 cm, then multiply the data in Table 1 by 0.5 to obtain the systems parameters for such a microscope.

When designing a microscope, it is generally necessary to determine the magnification required to enable the detector to record the smallest object features. For a two-mirror, multilayer reflecting microscope, it would be desirable to be able to record object features as small as 50 Å when operating within the water window. For a practical laboratory microscope, film should be used as a detector. Recently, Hoover, et al. [24] reported testing ten soft x-ray films with resolutions ranging from $120 - 5,000\ \frac{lp}{mm}$. It is also possible to use photoresist as a detector in the image plane with a capability of resolving image features as small as 100 Å. However, photoresist requires a contrast higher than most films for recording images. Therefore, systems based on using photoresist as a detector will not be considered any further here.

Using films with resolutions within the range of $2,000 - 5,000\ \frac{lp}{mm}$ to record object features as small as 50 Å will require a magnification of $50 - 20x$. Based on the data presented in Table 1, microscopes with magnifications of $40 - 50x$ are too long for convenient laboratory applications, unless the radius of curvature of the secondary mirror is very short, which creates other system fabrication problems. Therefore, a magnification ranging from $30 - 40x$ represents a compromise between competing factors, where the secondary mirror would have approximately a 5 cm radius of curvature.

To obtain a measure of the object plane resolution, one typically divides the image plane resolution (defined in terms of the system achieving a specified MTF which will account for the detector characteristics) by the system magnification. For microscope applications, it is convenient to use the object space numerical aperture, $NA(= \sin\theta)$, instead of the image space numerical aperture, $NA_{im}(= \sin u)$. However, from the Abbé Sine Condition

$$NA = m\ \ NA_{im}. \tag{4}$$

Equation 4 can be used to convert the numerical aperture from object to image space. In the following results, the object space NA is used as an independent variable. Figure 2 presents the sine wave MTF and point spread function (PSF) of a $30x$ Schwarzschild microscope. When different magnifications are considered, similar MTF and PSF plots can be made, but the object plane resolution is independent of the magnification.[26] However, the object plane resolution detoriates with increasing off-axis object points. Figure 3 presents the object plane resolution of a Schwarzschild microscope as a function of NA for different values of MTF. Note that an optimium object resolution is achieved for a NA within the range of $0.16 - 0.17$. The object resolution detoriates significantly for large NA, since the Schwarzschild microscope is only a third-order design.

When configuring a Schwarzschild microscope for a specific application,[25] it is desirable to understand the relationship between the numerical aperture (NA) of the microscope, the magnification (m), the diameter of the primary mirror ($D_{1,apt}$), and the radius of curvature of the secondary mirror (R_2). For a spherical Schwarzschild microscope, it follows from the definition $NA(\approx \sin\theta_{max})$ and Fig. 1:

$$NA = \frac{(D_{1,apt}/2)}{\sqrt{(D_{1,apt}/2)^2 + (Z_0 + R_1 - z_{1,max})^2}} \tag{5}$$

where from the equation of the primary mirror surface

$$z_{1,max} = \frac{(D_{1,apt}/2)^2}{R_1 + \sqrt{R_1^2 - (D_{1,apt}/2)^2}}. \tag{6}$$

Using Eqs. 5 and 6 for the calculations, Fig. 4 displays the relationship between NA, m, and the ratio $(D_{1,apt}/R_2)$. One notes from Fig. 4 that NA is a much stronger function of $(D_{1,apt}/R_2)$ than of the magnification of the system. For a practical example of the usefulness of the data presented in Fig. 4, consider that based on the object and detector resolutions, one seeks to build a $30x$ microscope with a NA of $0.3 - 0.4$, which based on the Rayleigh criterion:

$$Res = \frac{\lambda}{2\,NA} \tag{7}$$

would correspond to a resolution of $(1.2 - 1.6)\lambda$. Then, from Fig. 4, it follows that $(D_{1,apt}/R_2)$ would need to be within the range of $2.05 - 2.70$. It is generally recognized[21] that a spherical Schwarzschild microscope can not perform with diffraction limited resolution for a numerical aperture greater than approximately 0.17. But the aspherical Head microscope, which will be discussed in the next section, will enable operation of a reflecting microscope with diffraction limited resolution for a very large NA.

Figure 5 presents a plot of the object space NA versus R_2 for different values of $D_{1,apt}$. The relationships between these parameters should be considered before building a specific configuration of a two-mirror microscope. After a determination of m and NA, then substrate fabrication, polishing, and multilayer coating technologies will drive a determination of R_2 and $D_{1,apt}$. Also, it should be noted that a determination of first-order system parameters is required before the aspherical mirror shapes can be evaluated for a Head-Schwarzschild microscope which can provide diffraction limited performance for very large numerical apertures. For example, if one wishes to build a $30x$ microscope with a 12.5 cm diameter primary, then Fig. 5 predicts that R_2 would decrease from 5.9 cm to 4.5 cm as NA is increased from 0.3 to 0.4. More specifically, Table 1 and Fig. 5 predict the following first-order system parameters for a $30x$ microscope

$$NA = 0.35,\ L = 124.88\ cm,\ R_1 = 13.917\ cm,\ D_{1,apt} = 12.5\ cm,\ R_2 = 5\ cm. \tag{8}$$

A microscope with these system parameters can be fabricated with current technology. However, one must examine the aspherical surfaces required of this system to provide diffraction limited

resolution of $Res = \lambda/(2NA) = 1.4\lambda$. Also, one must evaluate the variation of the angle of incidence over both mirrors to determine the nature of the multilayer coatings which will be required.

3 Head-Schwarzschild Configuration

In order to improve the optical performance of a third-order design, such as the Schwarzschild microscope[12] or the conical microscope of Hannan[19], one often seeks an optical system which rigorously satisfies the Abbé Sine Condition:

$$\sin\theta = m \sin u \tag{9}$$

and the constant optical path length condition:

$$\rho + r + l = \rho_0 + r_0 + l_0 \tag{10}$$

where m is the microscope magnification, and the variables (ρ, r, l) are defined in Fig. 1. The constants (ρ_0, r_0, l_0) are the paraxial values of the corresponding variables. An optical system which satisfies Eqs. 9 and 10 is called an aplanat, which is free of all orders of spherical aberration and coma. In 1957, Head[22] presented an analytical solution in closed form for a two-mirror aplanat with finite object and image points, that is, a microscope or projection system. The primary and secondary mirror surfaces are specified by the following equations[20]:

Primary Microscope Mirror

$$\frac{l_0}{\rho} = \frac{(1+\kappa)}{2\kappa} + \frac{(1-\kappa)}{2\kappa}\cos\theta + \left(\frac{l_0}{\rho_0} - \frac{1}{\kappa}\right)\left(\frac{\gamma}{1+m}\right)^{-1}$$
$$* \left[\frac{\gamma-(1-m)}{2m}\right]^{\alpha}\left[\frac{\gamma-(m-1)}{2}\right]^{\beta}\left|\frac{(\kappa+1)\gamma}{2(m+1)} - \frac{(\kappa-1)}{2}\right|^{2-\alpha-\beta} \tag{11}$$

where $\kappa = (\rho_0 + r_0)/l_0$, $\alpha = m\kappa/(m\kappa - 1)$, $\beta = m/(m-\kappa)$, and $\gamma = \cos\theta + \sqrt{m^2 - \sin^2\theta}$.

Secondary Microscope Mirror

$$\frac{l_0}{r} = \frac{(1+\kappa)}{2\kappa} + \frac{(1-\kappa)}{2\kappa}\cos u + \left(\frac{l_0}{r_0} - \frac{1}{\kappa}\right)\left(\frac{\delta}{1+M}\right)^{-1}$$
$$* \left[\frac{\delta-(1-M)}{2M}\right]^{\alpha'}\left[\frac{\delta-(M-1)}{2}\right]^{\beta'}\left|\frac{(\kappa+1)\delta}{2(M+1)} - \frac{(\kappa-1)}{2}\right|^{2-\alpha'-\beta'} \tag{12}$$

where $M = 1/m$, $\alpha' = M\kappa/(M\kappa - 1)$, $\beta' = M/(M-\kappa)$, and $\delta = \cos u + \sqrt{M^2 - \sin^2 u} = M\gamma$. It is straight forward to evaluate the mirror profiles of a Head microscope from Eqs. 11 and 12 for

given input parameters ($m, r_0, l_0, and\ \rho_0$), which follow from Fig. 1 and Table 1 using the following correspondence between Schwarzschild and Head parameters:

$$(L - Z) \Longrightarrow \rho_0, \quad (R_1 - R_2) \Longrightarrow l_0, \quad (L - Z_0 - R_2) \Longrightarrow r_0.$$

In order to use a conventional optical design program to analyze the performance of a Head microscope, it is necessary to fit an equation to the numerical surface data representing the primary and secondary mirror surfaces. There are many ways to describe optical surfaces. Normally, optical surfaces are described by an equation with a conic term plus some aspherical deformation terms:

$$z = \frac{ch^2}{1 + \sqrt{1 - (1 + \kappa)c^2h^2}} + \sum_{i=2}^{n} A_{2i}h^{2i} \tag{13}$$

where h is the radial distance of a point on the surface from the symmetry axis, $c(= 1/R)$ is the curvature of the vertex of the mirror, κ is the conic constant, and A_{2i} are the aspherical deformation coefficients. If κ and A_{2i} are zero, then Eq. 13 specifies that the surface is a sphere. If κ is not zero, but all A_{2i} are zero, then Eq. 13 represents a conical surface.

After evaluating the surface data for the primary and secondary mirrors in a Head microscope from Eqs. 11-12, then we have used both linear and nonlinear least squares fitting algorithms to determine the surface parameters of Eq. 13 such that the Head microscope can be very consistently modeled to satisfy the aplanatism conditions and to yield diffraction limited resolution for the desired NA. For a specific set of surface data, it is not clear initially how many aspherical deformation terms will be required or whether the conic constant is zero. Experience has shown that it is desirable to determine an approximate shape of the Head surfaces before doing extensive nonlinear least squares fitting. As a result of the initial values used in this work, the Head surfaces can be approximated by spherical Schwarzschild microscope surfaces with the corresponding surface parameters. Good representations for Head surfaces have been determined to have a small conic constant and one to two aspherical deformation terms or to have zero conic constant with four to eight aspherical deformation terms. It has been found[27] that there are no unique representations for the fitting of a Head microscope surface, but all well behaved solutions have the same diffraction limited optical performance. Reference [27] presents Head surface parameters for a number of very well fit $30x$ and $40x$ microscopes which can provide diffraction limited performance for very large numerical apertures.

For example, using a nonlinear least squared fitting algorithm, a set of Head surface parameters is given in Table 2 for a $30x$ microscope with $NA = 0.35$ where the following axial spacings have been used

$$d_0 = 90.318625\ mm,\ d_1 = 89.1710\ mm,\ d_2 = 1159.5595\ mm. \tag{14}$$

Typical aspherical surfaces described in Table 2 and Ref. [27] differ from a spherical surface by approximately one micron for a primary aperture radius of 70 mm, which corresponds to a $NA = 0.35$. Figure 6 displays the deviation of the Head microscope surface from the best fit spherical surfaces as a function of the aperture radius for the microscope with system parameters given by Eq. 8 and Table 2 or Ref. [27]. Current substrate fabrication technologies should be able to make the mirror surfaces defined by Table 2. The MTF for the systems given in Eq. 8 and Table 2 or

Ref. [27] are diffraction limited for small objects with diameters ranging from $40 - 50\ \mu m$ with results similar to those shown in Fig. 2, but with different cutoff frequencies.

A challenging application for soft x-ray optics is to develop a multilayer, reflecting system which operates within the water window ($23 - 44$ Å) [4, 9, 28] and which can provide higher resolution than a spherical zone plate microscope (300 Å) or a spherical Schwarzschild configuration. Figure 7 compares the object resolution of a $30x$ spherical Schwarzschild and Head microscope to the diffraction limited performance as a function of NA for an on-axis object. Since a Head microscope rigorously satisfies the Abbé Sine Condition and the constant optical path length condition, one expects that a Head microscope should be diffraction limited for on-axis objects, as shown in Fig. 7. Therefore, one can project from Eq. 7 that the theoretical resolution of a Head microscope would approach $1.2 - 1.6\ \lambda$ when operating with a NA of $0.3 - 0.4$. Figure 8 presents the off-axis performance of a Head microscope as a function of NA. If an image can be recorded with a MTF of 0.2, then the modeling results presented in Fig. 8 predict that the Head microscope should provide a resolution of 30 Å over the entire object of 40 μm diameter, which exceeds the Rayleigh criterion for resolution given by Eq. 7 that requires a higher MTF at the half-cutoff frequency. It should be noted that these results are based on an *idealized configuration* without taking into account requirements which multilayer coatings impose on the reflectivity or of substrate and system fabrication tolerances. Also, this work has not addressed the practical issues of potential radiation demage of the object.

Next, it is important to determine whether it is possible to deposit multilayer coatings on these fast mirror surfaces. Figure 9 presents the variation of the angle of incidence on both the primary and secondary Head mirrors as a function of the microscope NA for the $30x$ Head microscope which is defined by Eq. 8 and Table 2, where the diameter of the primary was increased to achieve a larger numerical aperture. It is evident from Fig. 9 that the angle of incidence varies more rapidly over the secondary than the primary. This strong variation of the angle of incidence over the secondary mirror has significant implications for the design and fabrication of multilayer coatings for a fast Head microscope. Depending on how a multilayer is designed, peak reflectivities may only be maintained for a $5 - 10°$ variation in the angle of incidence over the multilayer. Therefore, conventional multilayer coatings can not be used for a very fast Head microscope. However, graded or segmented multilayer coatings may be used to coat the secondary mirror such that operation with acceptable reflectivity may be achieved for a wide range of numerical apertures.[25] In the next section, results of system tolerances and surface contour error analysis will be presented.

4 Tolerance Analysis: Schwarzschild and Head Results

Results from the previous two sections have indicated that a spherical Schwarzschild microscope should be able to provide a diffraction limited resolution of 3.3λ and that a Head microscope operating with $NA = 0.35$ should be able to provide a diffraction limited resolution of 1.4λ. In this section, results of a conventional tolerance analysis are presented. Specifically, the optical performance of a spherical Schwarzschild microscope configured to operate with $\lambda = 40$ Å and

130 Å have been analyzed, where the effects of introducing perturbations in the design values of the mirror separation, radii of curvature, tilt and decentration of the primary and secondary mirrors are considered. Three levels of tolerance analysis have been determined which will prevent the image space MTF(im) at the half-cutoff frequency from dropping below 0.20, 0.15, and 0.10, respectively. Table 3 summarizes these results for a spherical Schwarzschild microscope operating at 130 Å, and Table 4 presents similar results for a spherical Schwarzschild microscope operating at 40 Å. Results from Tables 3 and 4 indicate that there will be very tight tolerances required on the fabrication and assembly of a Schwarzschild soft x-ray microscope where the tolerances at 40 Å will be approximately $2-3$ times greater than those required for similar performance for a system operating at 130 Å. It also follows that tolerances associated with the secondary mirror are more stringent than those required of the primary mirror for similar performance.

In order to assess the importance of surface contour errors on system performance, we have evaluated the effect of surface perturbations to the Head microscope system. These surface perturbations have been constructed such that there is not any deviation from the Head surfaces for axial points and that the perturbations oscillate with increasing amplitute for peripheral points. Specifically, the sag as a function of the radial coordinate h of the perturbed Head surface is given by

$$Z = Z_H + \Delta Z \tag{15}$$

where Z_H can be determined for the primary and secondary mirrors from Eqs. 11 and 12. The surface perturbation has been assumed to be in the specific form

$$\Delta Z = \Delta Z_{\max} [1 + 0.05 \sin(2\pi f h)] \left(\frac{h}{h_{\max}}\right). \tag{16}$$

Figure 10 displays a perspective view of a Head microscope mirror surface with a surface perturbation and a cross-sectional view of the surface perturbation for different values of f. Specific values for f and $\Delta Z_{\max}$ have been determined empirically to illustrate when the system MTF(im) significantly detoriates due to these surface contour errors. Figures 11 and 12 display the MTF(im) of Head microscope with surface contour errors for different wavelengths. From these results it is apparent that for f greater than $(8/h_{\max})$ then the MTF(im) has degraded significantly. Also, for water window operation the peak-to-valley($2\ \Delta Z_{\max}$) surface contour errors should be kept less than 50 Å at peripheral points on the mirror surfaces. Whereas, the peak-to-valley surface contour errors should be less than 200 Å for operations with 130 Å soft x-rays. These results indicate that achieving near diffraction limited performance within the water window will push the state-of-art in substrate fabrication and system assembly.

5 Conclusions

This work has summarized for a Schwarzschild microscope some relationships between NA, magnification, diameter of the primary mirror, radius of curvature of the secondary mirror, and the total length of the microscope. To achieve resolutions better than a spherical Schwarzschild microscope of 3.3λ for a perfectly aligned and fabricated system, it is necessary to use aspherical surfaces to control higher-order aberrations. For a NA of 0.35, the aspherical Head microscope provides diffraction limited resolution of 1.4λ where the aspherical surfaces differ from the best fit spherical surface by approximately 1 micron. However, the angle of incidence varies significantly over the primary and the secondary mirrors, which will require graded multilayer coatings to operate near peak reflectivities. For higher numerical apertures, the variation of the angle of incidence over the secondary mirror surface becomes a serious problem which must be solved before multilayer coatings can be used for this application. Tolerance analysis of the spherical Schwarzschild microscope has shown that water window operations will require $2-3$ times tighter tolerances to achieve a similar performance for operations with 130 Å radiation. Surface contour errors have been shown to have a significant impact on the MTF and must be controlled to a peak-to-valley variation of $50-100$ Å and a frequency of 8 periods over the surface of a mirror.

6 Acknowledgements

The authors would like to express gratitude to the NASA/MSFC Center Director's Discretionary Fund, NASA/MSFC Technology Utilization Office, and to the University of Alabama at Birmingham for partial support of this research.

References

[1] *X-Ray Microscopy*, G. Schmal and D. Rudolph, Eds., Springer Series in Optical Sciences, vol. 43 (Springer-Verlag, New York, 1984).

[2] *X-Ray Microscopy II*, D. Sayre, M. Howell, J. Kirz, and H. Rarback, Eds., Springer Series in Optical Sciences, vol. 56 (Springer-Verlag, New York, 1987).

[3] *X-Ray Microscopy III*, A.G. Michette, G. R. Morrison, and C. J. Buckley, Eds., Springer Series in Optical Sciences, vol. 67 (Springer-Verlag, New York, 1990).

[4] M. R. Howells, J. Kirz, and D. Sayre, "X-ray microscopes," Sci. Am., 88-94, February, 1991.

[5] T. W. Barbee, Jr., "Multilayers for x-ray optical applications," in *X-Ray Microscopy*, G. Schmal and D. Ruldolph, Eds.,Springer Series in Optical Sciences, vol. 43 (Springer-Verlag, New York, 1984), 144-162.

[6] E. Spiller, "Enhancement of the reflectivity of multilayer x-ray mirrors by ion-polishing," Proc. SPIE **1160**, 271-279 (1989).

[7] R. A. London, M. D. Rosen, and J. E. Trebes, "Wavelength choices for soft-x-ray laser holography for biological sample," Appl. Opt. **28**, 3397-3404(1989).

[8] J. A. Trail, *A Compact Scanning Soft X-Ray Microscope*, Ph. D. Dissertation, Stanford University (1989).

[9] R. B. Hoover, D. L. Shealy, B. R. Brinkley, P. C. Baker, T. W. Barbee, Jr., and A. B. C. Walker, Jr., "X-ray imaging microscope for cancer research," in *Technology 2000*, NASA Conference Publication 3109, vol. 1, 73-82 (1991).

[10] R. B. Hoover, D. L. Shealy, B. R. Brinkley, P. C. Baker, T. W. Barbee, Jr., and A. B. C. Walker, Jr., "Development of the water window imaging x-ray microscope utilizing normal-incidence multilayer layer optics," Opt. Eng. **30.8**, 1086-1093 (1991).

[11] K. Schwarzschild, "Untersuchungen zur geometrischen Optik, II; Theorie der Spiegelteleskope," Abh. der Königl. Ges. der Wiss. zu Göttingen, Math.-phys. Klasse, 9. Folge, Bd IV, No. 2 (1905).

[12] D.L. Shealy, D. R. Gabardi, R. B. Hoover, A. B. C. Walker, Jr., J. F. Lindblom, and T. W. Barbee, Jr., "Design of a normal incidence multilayer imaging x-ray microscope," J. X-Ray Sci. Technol. **1**, 190-206 (1989).

[13] R. B. Hoover, P. C. Baker, D. L. Shealy, D. B. Gore, A. B. C. Walker, Jr., T. W. Barbee, Jr., and T. Kerstetter, "Imaging Schwarzschild multilayer x-ray microscope," NASA - Marshall Space Flight Center, Space Science Laboratory Preprint Series No. 92-124 (Huntsville, AL, December, 1992).

[14] E. Spiller, "A scanning soft x-ray microscope using normal incident mirrors," in *X-Ray Microscopy*, G. Schmal and D. Rudolph, Eds., Springer Series in Optical Sciences, vol. 43 (Springer-Verlag, New York, 1984), 226-231.

[15] J. H. Underwood, R. C. C. Perera, J. B. Kortright, P. J. Batson, C. Capasso, S. H. Liang, W. Ng, A. K. Ray-Chaudhuri, R. K. Cole, G. Chen, Z. Y. Guo, J. Wallace, J. Welnak, G. Margaritondo, F. Cerrina, G. De Stasio, D. Mercanti, and M. T. Ciotti, "The MAXIMUM photoelectron microscope at the University of Wisconsin's Synchrotron Radiation Center," in *X-Ray Microscopy III*, A.G. Michette, G. R. Morrison, and C. J. Buckley, Eds., Springer Series in Optical Sciences, vol. 67 (Springer-Verlag, New York, 1990), 220-225.

[16] R. P. Haelbich, "A scanning ultrasoft x-ray microscope with multilayer coated reflection optics: first test with synchrotron radiation around $50eV$ photon energy," in *Scanned Image Microscope*, Ash, Ed. (1981), 413.

[17] D. W. Berreman, J. E. Bjorkholm, L. Eichner, R. R. Freeman, T. E. Jewell, W. M. Mansfield, A. A. MacDowell, M. L. O'Malley, E. L. Raab, W. T. Silfvast, L. H. Szeto, D. M. Tennant, W.

K. Waskiewicz, D. L. White, D. L. Windt, and O. R. Wood II, "Reduction imaging at 14nm using multilayer-coated optics: printing of features smaller than 0.1μm," J. Vac. Sci. Technol. B 8.6, 1509-1513 (1990).

[18] H. Kinoshita, K. Kurlhara, Y. Ishll, and Y. Torii, "Soft-x-ray reduction lithography using multilayer mirrors," J. Vac. Sci. Technol. **B 7.6**, 1648-1651 (1989).

[19] P. G. Hannan, "General analysis of two-mirror relay systems," Appl. Opt. **31.4**, 513-518 (1992).

[20] D. L. Shealy, W. Jiang, and R. B. Hoover, "Design and analysis of aspherical multilayer imaging x-ray microscope," Opt. Eng. **30.8**, 1094-1099 (1991).

[21] D. L. Shealy, C. Wang, W. Jiang, and R. B. Hoover, "Design and analysis of soft-x-ray imaging microscopes," Proc. SPIE **1546**, 117-124 (1991).

[22] A. K. Head, "The two-mirror aplanat," Proc. Phys. Soc. **LXX, 10-B**, 945-949 (1957).

[23] P. Erdös, "Mirror anastigmat with two concentric spherical surfaces," JOSA **49.9**, 877 (1957).

[24] R. B. Hoover, A. B. C. Walker, Jr., C. E. DeForest, R. Watts, and C. Tarrio, "Ultrahigh resolution photographic films for x-ray/EUV/FUV Astronomy," NASA - Marshall Space Flight Center, Space Science Laboratory Preprint Series No. 92-125 (Huntsville, AL, December, 1992).

[25] D. L. Shealy, C. Wang, W. Jiang, L. Jin, and R. B. Hoover, "Design and analysis of a fast, two-mirror soft-x-ray microscope," Proc. SPIE **1741**, 20-31 (1992).

[26] D. L. Shealy, R. B. Hoover, T. W. Barbee, Jr., and A. B. C. Walker, Jr., "Design and analysis of a Schwarzschild imaging multilayer x-ray microscope," Opt. Eng. **29.7**, 721-727 (1990).

[27] D. L. Shealy, C. Wang, W. Jiang, and J. Lin, "Final Report 1992: Advanced Water Window X-Ray Microscope Design and Analysis," NASA - Marshall Space Flight Center, Purchase Order No. H-08073D (Birmingham, AL, September 11, 1992).

[28] R. B. Hoover, D. L. Shealy, B. R. Brinkley, P. C. Baker, T. W. Barbee, Jr., and A. B. C. Walker, Jr., "Development of the water window imaging x-ray microscope utilizing normal-incidence multilayer optics," Opt. Eng. **30.8**, 1086-1093 (1991).

$M(x)$	$R_1(cm)$	$Z_0(cm)$	$Z(cm)$	$L(cm)$
2	109.0833	8.256939	-92.5694	117.3402
3	58.2843	8.047379	-34.1421	66.3316
4	45.5840	8.006406	-13.5584	53.5904
5	40.0000	8.000000	0.0	48.0000
10	31.7929	8.023756	48.4446	88.2613
20	28.7361	8.052073	132.3053	169.0935
30	27.8342	8.063728	214.0777	249.9756
40	27.4027	8.069952	295.3954	330.8680
50	27.1497	8.073812	376.5409	411.7644
60	26.9835	8.076437	457.6027	492.6626
70	26.8659	8.078337	538.6176	573.5619
80	26.7784	8.079775	619.6036	654.4618
90	26.7107	8.080902	700.5705	735.3621
100	26.6567	8.081809	781.5242	816.2627

Table 1: Schwarzschild Microscope Parameters for $R_2 = 10cm$.

Variable	Primary	Secondary
Diameter(mm)	140.0	29.0
Hole Dia. (mm)	30.0	none
Vertex Radius (mm)	139.170963	49.999915
Conic Constant	0.0029751487	-0.002862214
A4 (mm-3)	1.405927D-10	-1.826711D-9
A6 (mm-5)	0	-4.739086D-11

Table 2: Surface parameters for a $30x$ Head microscope.

Variable	Design Value	Tolerance: MTF(im) at half-cutoff frequency		
		≥ 0.200	≥ 0.150	≥ 0.100
R_1	139.170963 mm	0.140 μm	0.185 μm	0.230 μm
Tilt of S_1	0.00000 rad	1.152 $mrad$	1.340 $mrad$	1.500 $mrad$
Decenter of S_1	0.00000 mm	180.0 μm	215.0 μm	238.0 μm
R_2	50.00004 mm	0.360 μm	0.490 μm	0.610 μm
Tilt of S_2	0.00000 rad	0.105 $mrad$	0.136 $mrad$	0.166 $mrad$
Decenter of S_1	0.00000 mm	5.400 μm	6.900 μm	8.500 μm
Spacing	89.1710 mm	0.180 μm	0.235 μm	0.290 μm

Table 3: Tolerance analysis of a $30x$ Schwarzschild microscope with $NA = 0.15$ and $\lambda = 130$ Å.

Variable	Design Value	Tolerance: MTF(im) at half-cutoff frequency		
		≥ 0.200	≥ 0.150	≥ 0.100
R_1	139.170963 mm	0.030 μm	0.059 μm	0.075 μm
Tilt of S_1	0.00000 rad	0.611 $mrad$	0.698 $mrad$	0.785 $mrad$
Decenter of S_1	0.00000 mm	95.00 μm	112.0 μm	128.0 μm
R_2	50.00004 mm	0.090 μm	0.135 μm	0.180 μm
Tilt of S_2	0.00000 rad	0.030 $mrad$	0.040 $mrad$	0.051 $mrad$
Decenter of S_1	0.00000 mm	1.500 μm	2.000 μm	2.530 μm
Spacing	89.1710 mm	0.050 μm	0.065 μm	0.085 μm

Table 4: Tolerance analysis of a $30x$ Schwarzschild microscope with $NA = 0.15$ and $\lambda = 40$ Å.

Figure Captions

Figure 1: Geometrical configuration of a Head-Schwarzschild microscope.

Figure 2: Sine Wave MTF and PSF of a $30x$ Schwarzschild microscope.

Figure 3: Object plane resolution of a spherical Schwarzschild microscope as a function of NA.

Figure 4: Numerical aperture of spherical Schwarzschild microscope as a function of the normalized primary mirror diameter ($D_{1,apt}/R_2$) for different magnifications.

Figure 5: Numerical aperture of a $30x$ spherical Schwarzschild microscope as a function of the secondary radius of curvature (R_2) for different diameters of the primary mirror ($D_{1,apt}$).

Figure 6: Deviation of Head microscope surfaces from the best fit spherical surface.

Figure 7: Comparsion of the object resolution between Schwarzschild and Head microscopes as a function of the object space NA.

Figure 8: Comparsion of the object resolution of a Head microscope as a function of the object space NA for different object heights.

Figure 9: Variation of the angle of incidence over the $30x$ Head microscope surfaces as a function of numerical aperture.

Figure 10: Perturbed Head microscope surface: (a) Perspective view and (b) Cross-sectional view for different spatial frequencies of contour errors.

Figure 11: MTF(im) of Head microscope system for different surface contour errors.

Figure 12: MTF(im) of Head microscope system for different surface contour errors.

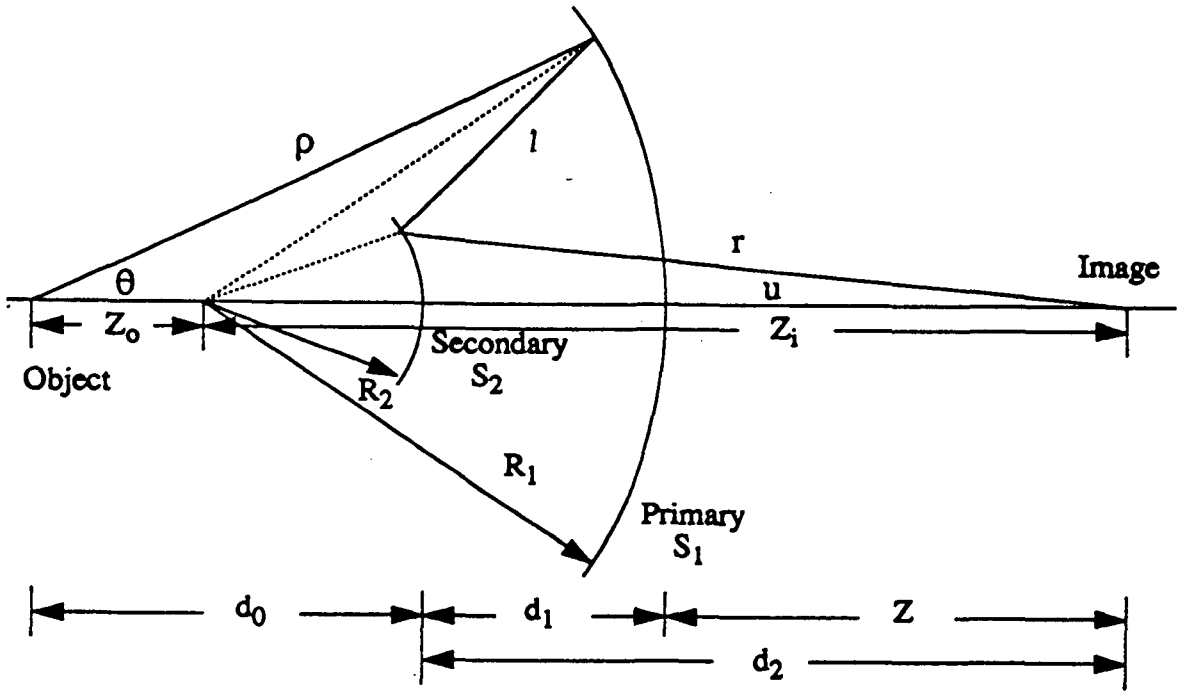

Figure 1: Geometrical configuration of a Head-Schwarzschild microscope.

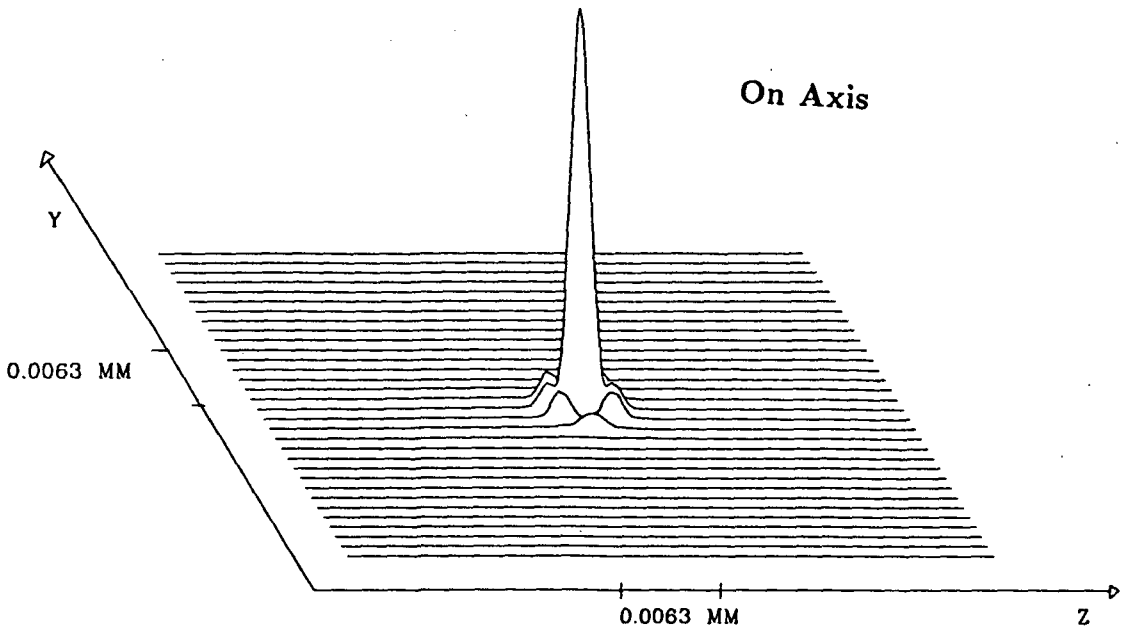

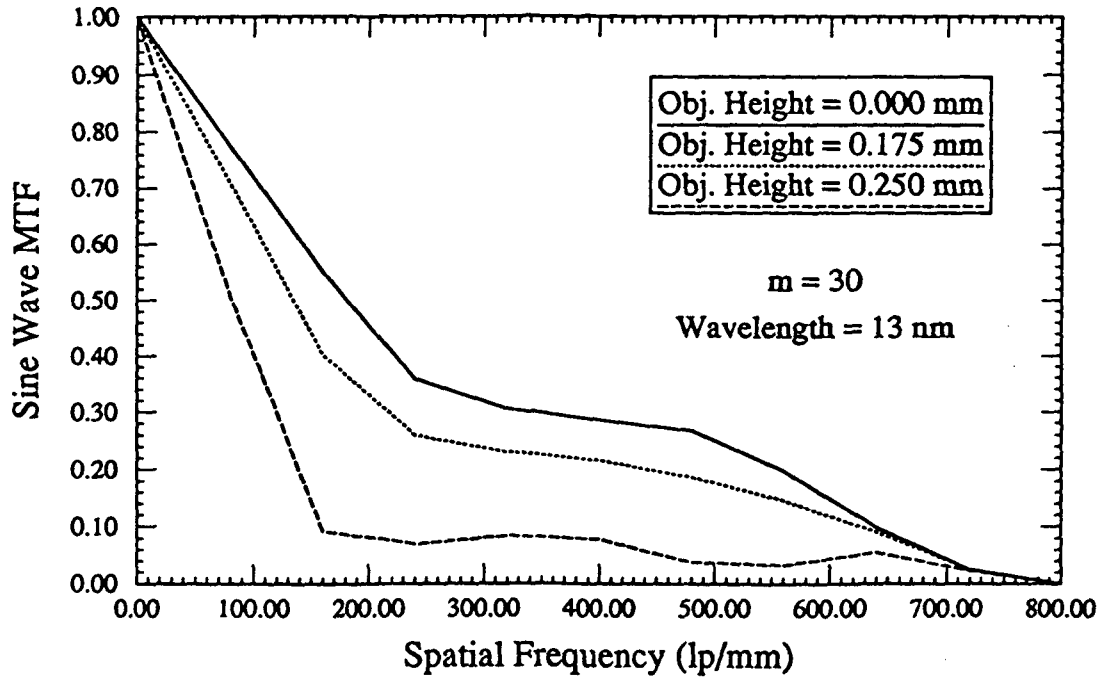

Figure 2: Sine Wave MTF and PSF of a 30x Schwarzschild microscope.

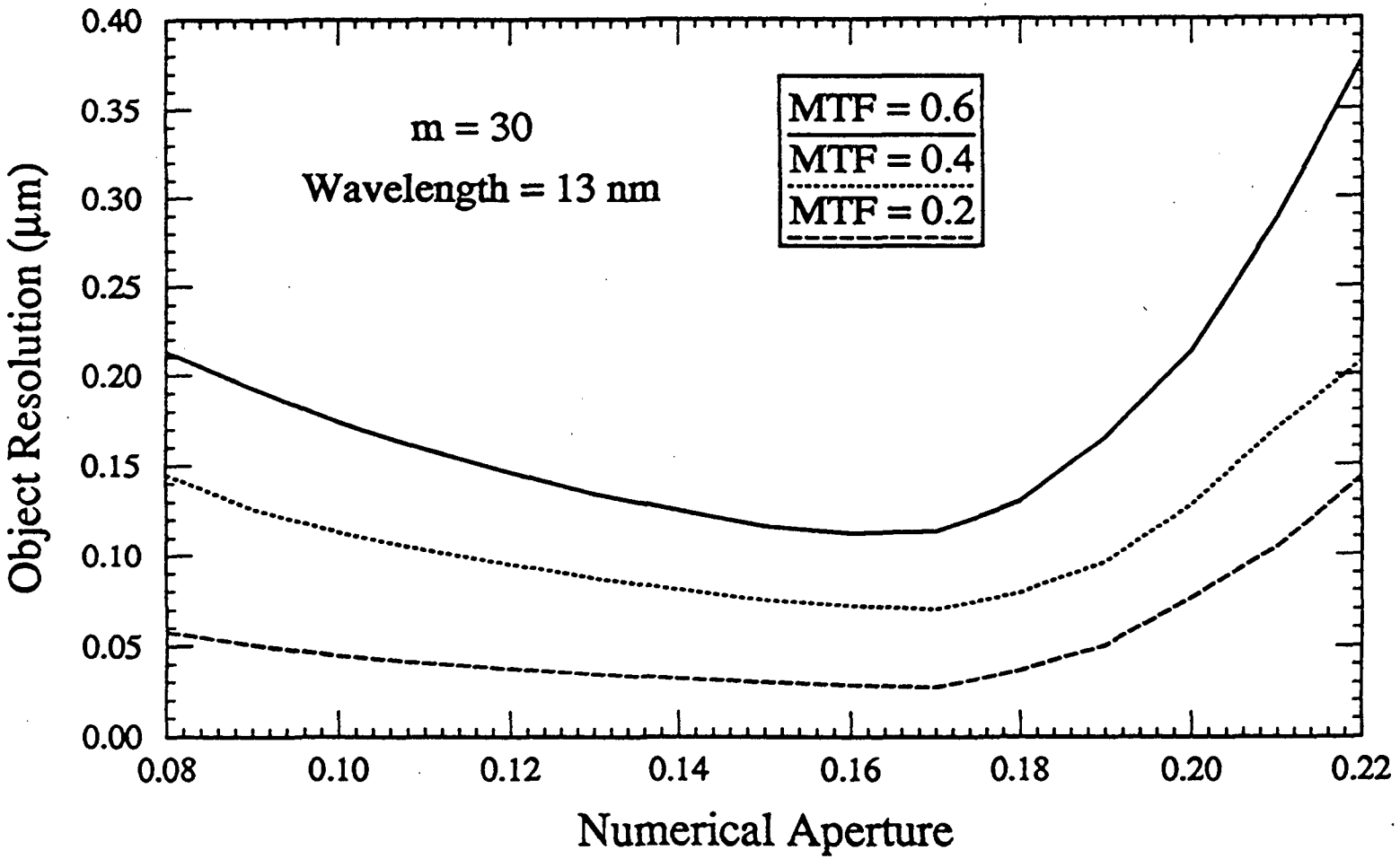

Figure 3: Object plane resolution of a spherical Schwarzschild microscope as a function of NA.

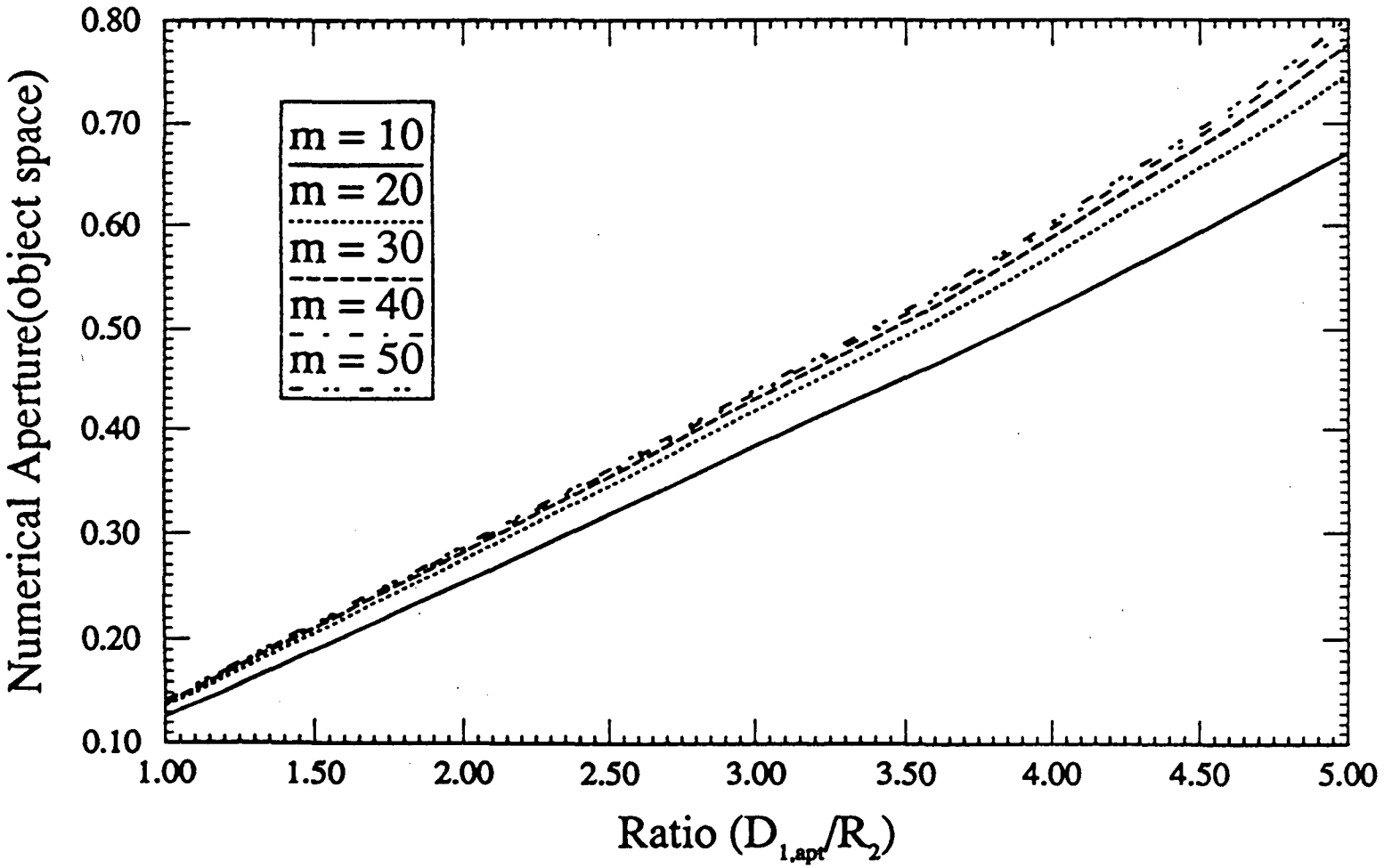

Figure 4: Numerical aperture of spherical Schwarzschild microscope as a function of the normalized primary mirror diameter ($D_{1,apt}/R_2$) for different magnifications.

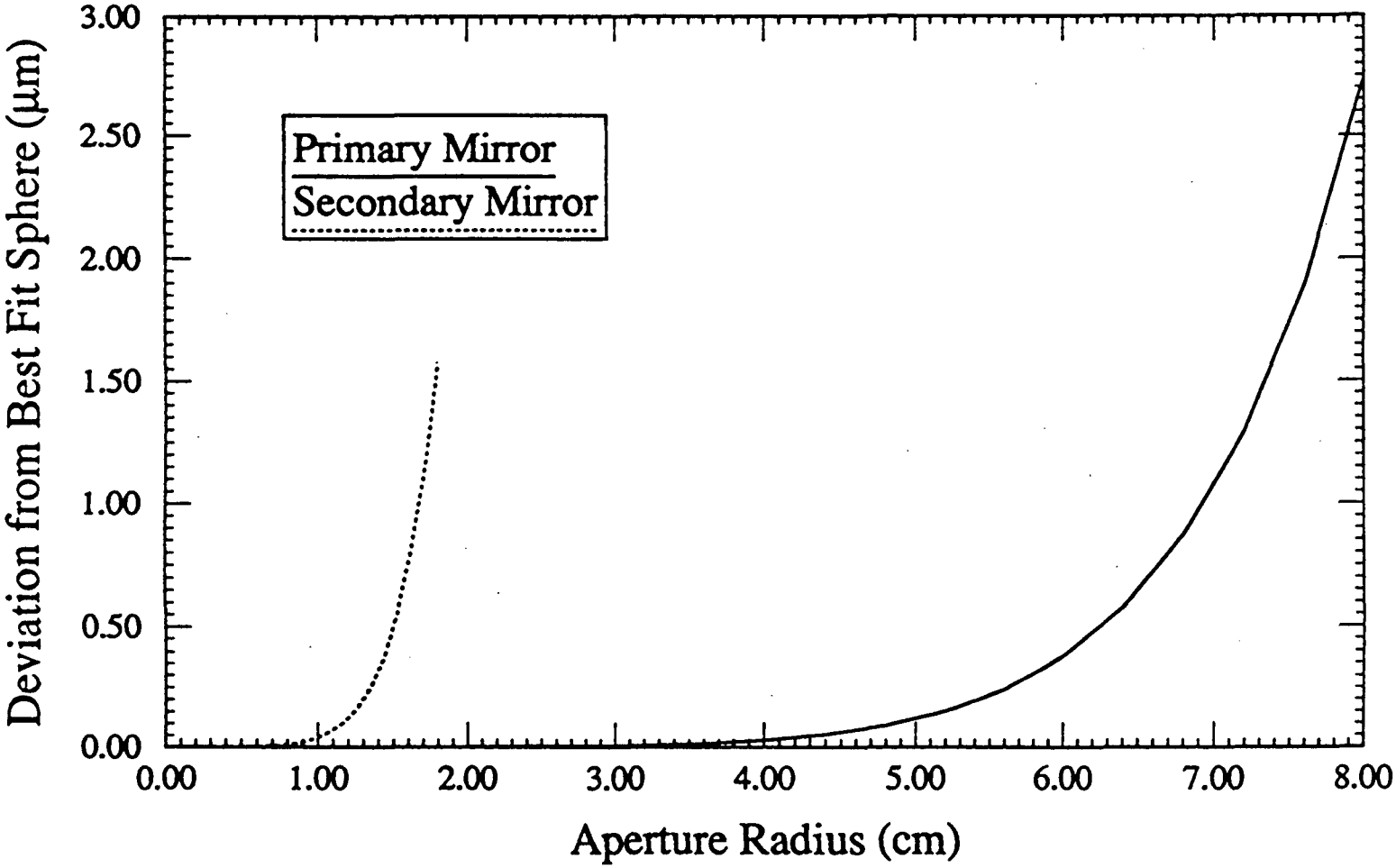

Figure 6: Deviation of Head microscope surfaces from the best fit spherical surface.

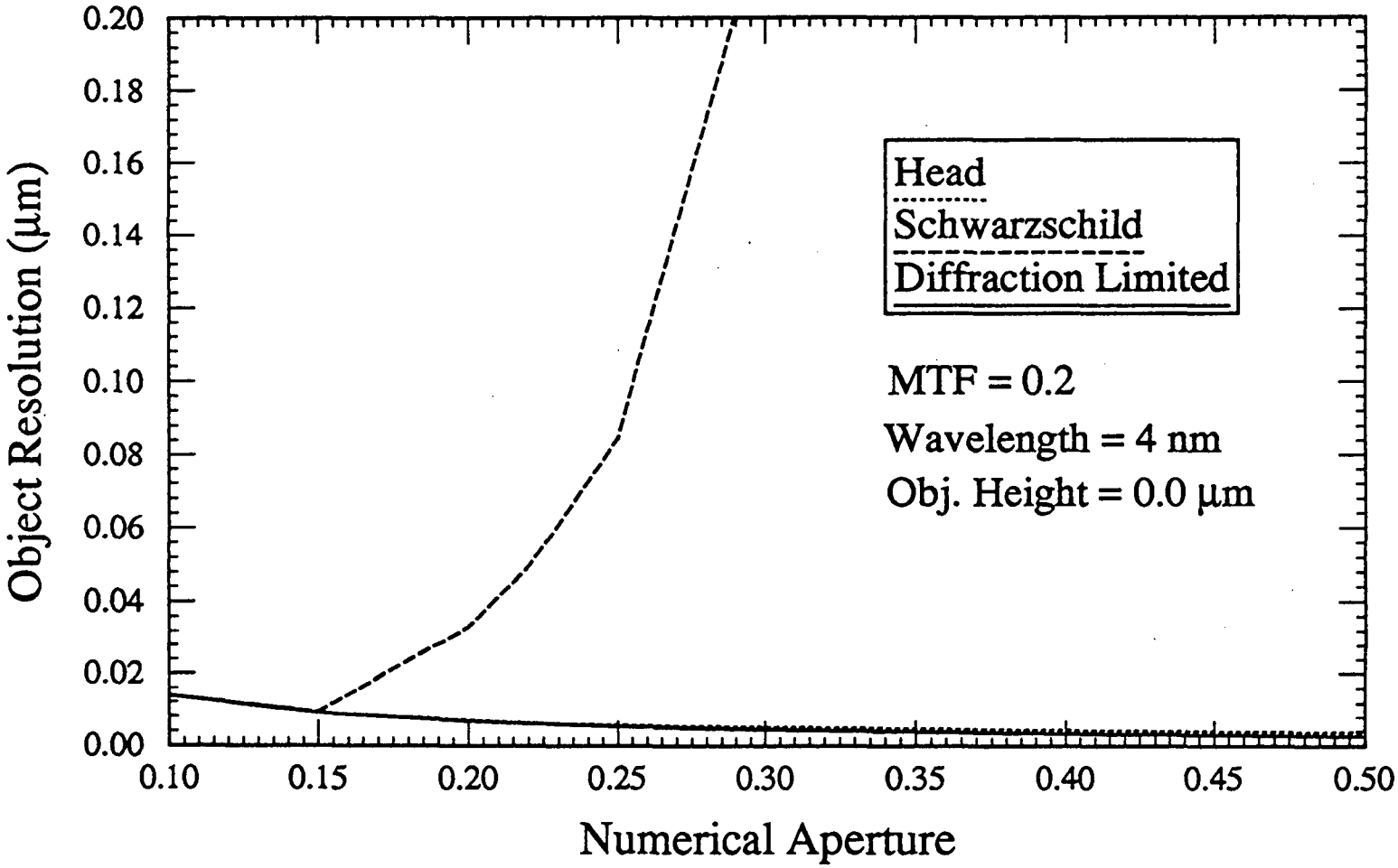

Figure 7: Comparsion of the object resolution between Schwarzschild and Head microscopes as a function of the object space NA.

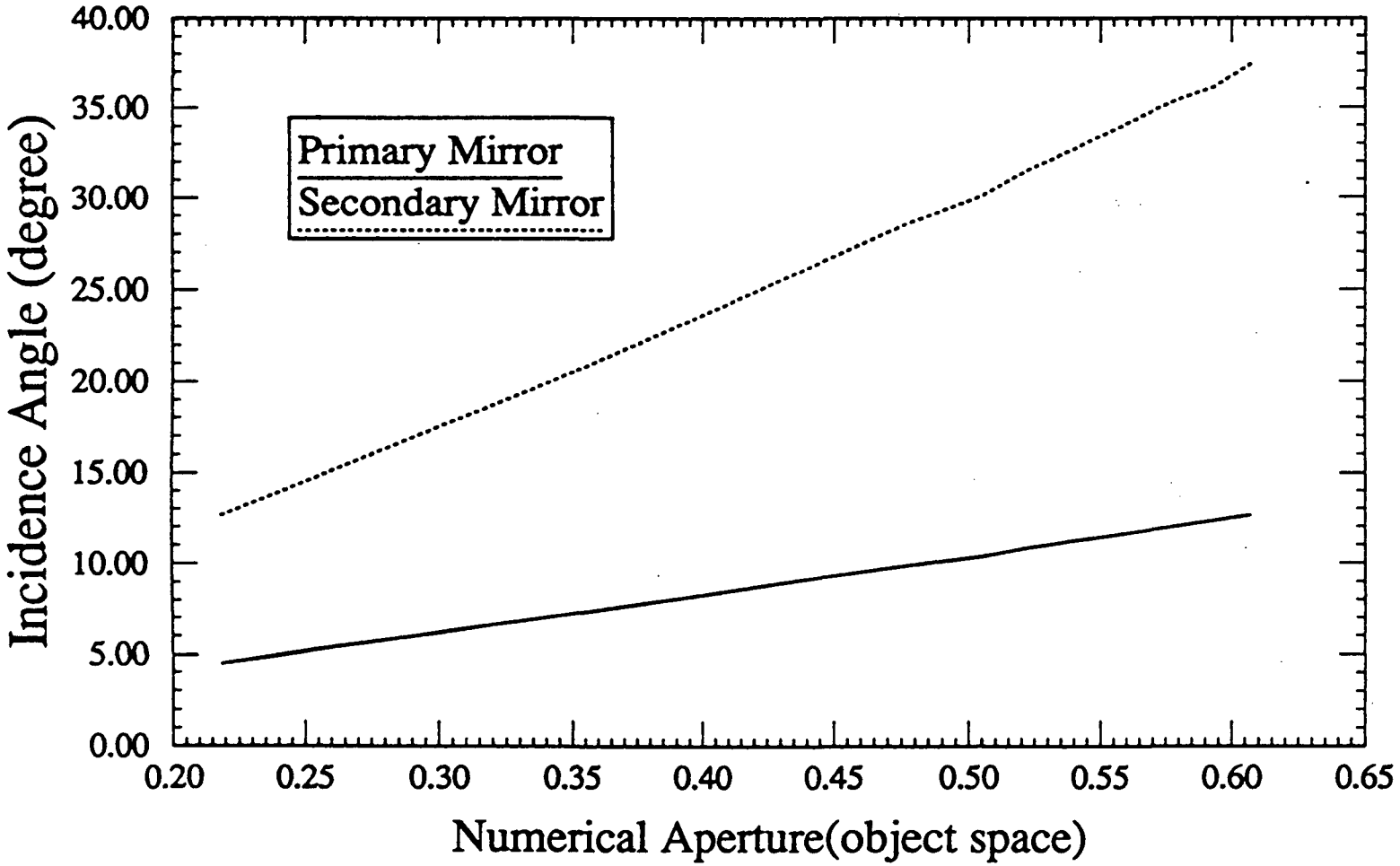

Figure 9: Variation of the angle of incidence over the $30x$ Head microscope surfaces as a function of numerical aperture.

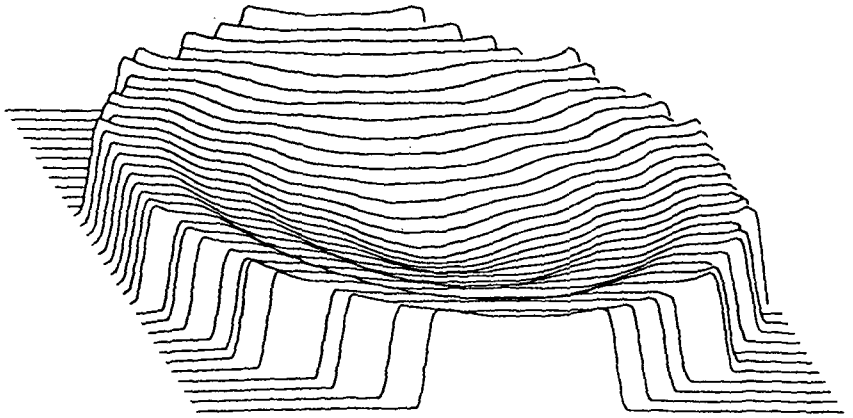

A

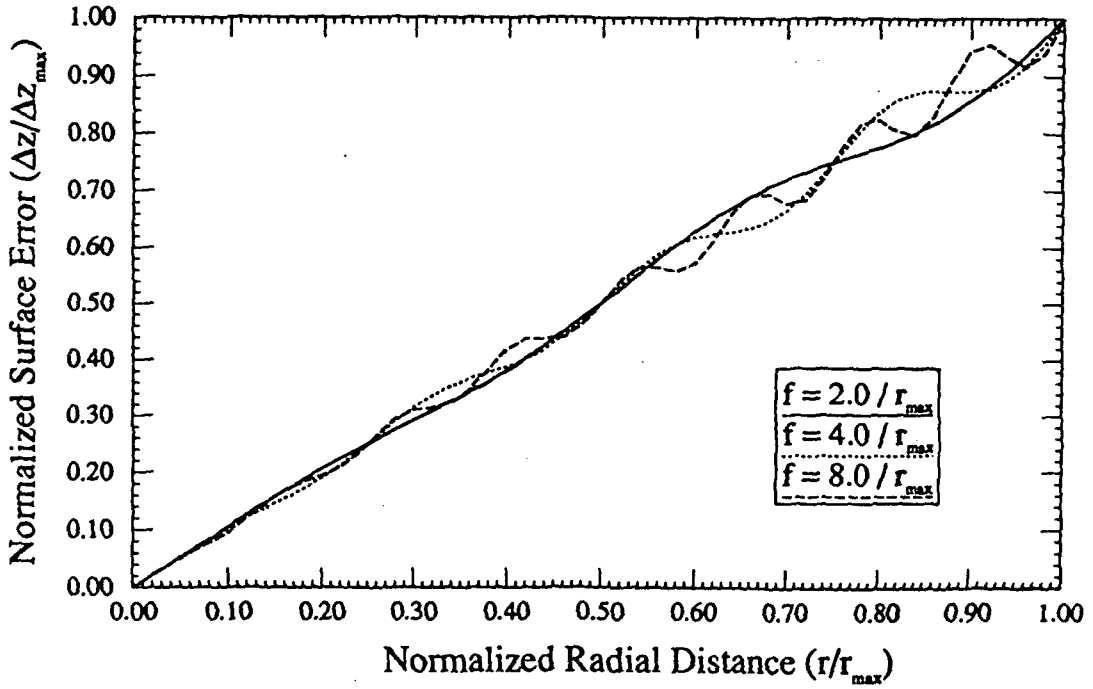

B

Figure 10: Perturbed Head microscope surface: (a) Perspective view and (b) Cross-sectional view for different spatial frequencies of contour errors.

MTF Analysis for a 30x Head Microscope with Surface Errors

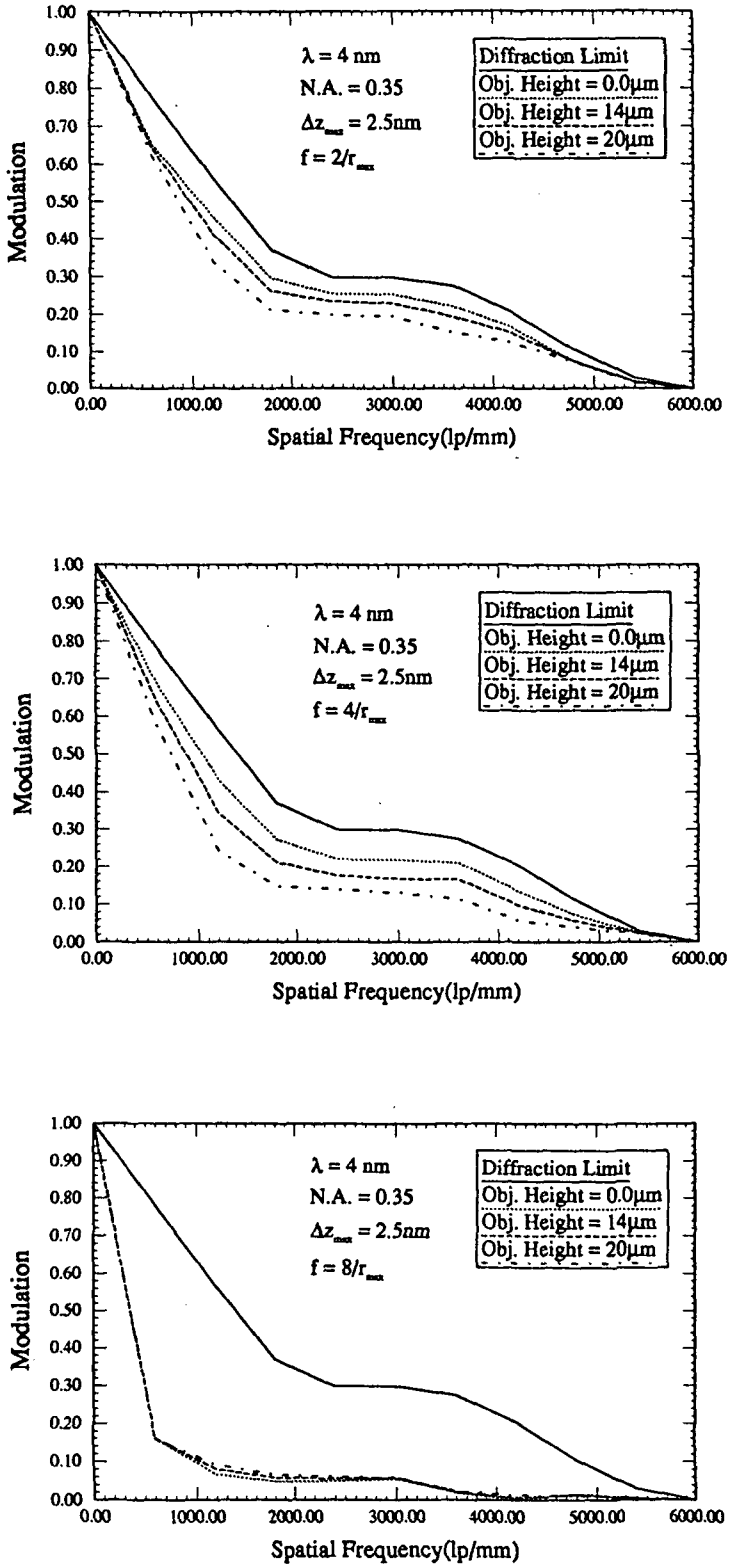

Figure 11: MTF(im) of Head microscope system for different surface contour errors.

MTF Analysis for a 30x Head Microscope with Surface Errors

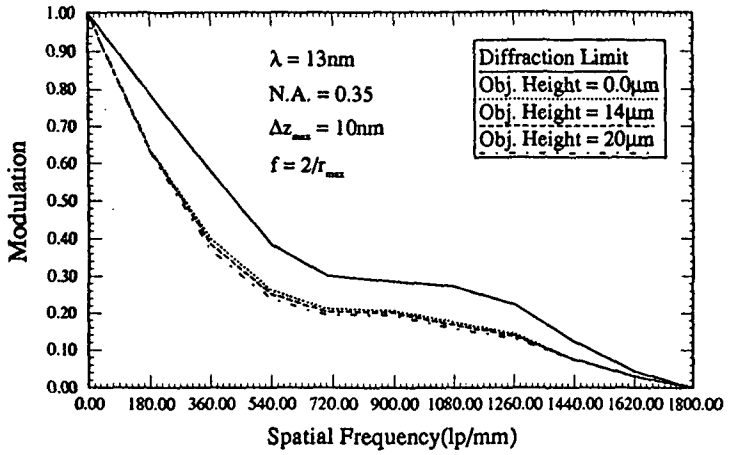

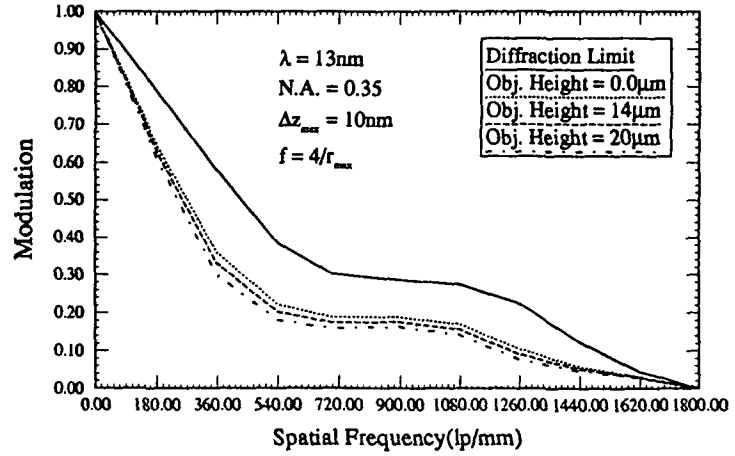

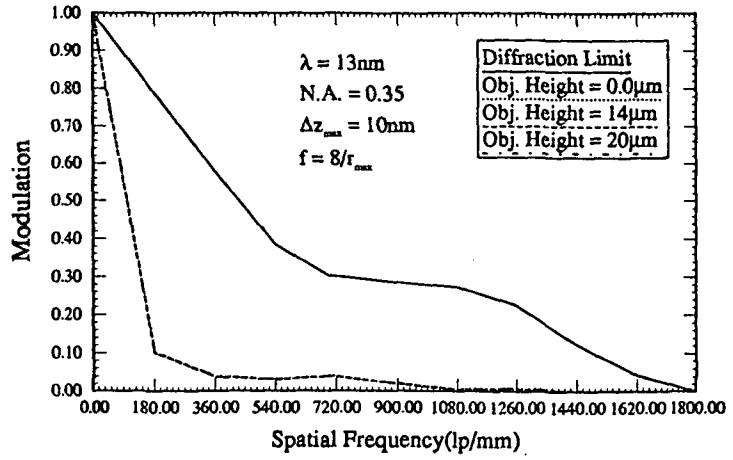

Figure 12: MTF(im) of Head microscope system for different surface contour errors.